Pergamon

Geochimica et Cosmochimica Acta, Vol. 68, No. 18, pp. 3643–3656, 2004

0016-7037/04 $30.00 + .00

doi: 10.1016/j.gca.2004.03.017

Effects of photoirradiation on the adsorption of dissolved organic matter to goethite

MICHAEL J. PULLIN,† CHRISTINA A. PROGESS and PATRICIA A. MAURICE*
Dept. of Civil Engineering and Geological Sciences, University of Notre Dame, Notre Dame, IN 46556 USA

(*Received October* 9, 2003; *accepted in revised form March* 16, 2004)

Abstract—The effects of photoirradiation of dissolved organic matter (DOM) on its subsequent adsorption to the Fe(III)oxyhydroxide mineral goethite were investigated at 22°C in 0.10 mol L^{-1} $NaClO_4$ solutions at pH 3.5 and 5.5, Photoirradiation of DOM decreased the abundance of high molecular-weight components and formed new lower molecular-weight components, including low molecular weight carboxylic acids (i.e., formic, malonic, and acetic acids). Adsorption of non-irradiated DOM decreased from pH 3.5 to 5.5 and was dominated by the intermediate molecular weight (1251–3750 Da) fraction, although the 451–1250 and 3751–11350 Da fractions also contributed to adsorption at pH 3.5. Irradiation resulted in a substantial decrease in DOM adsorption affinity at pH 3.5, primarily due to loss of components in the 1251–3750 and 3751–11350 Da fractions. Irradiation resulted in only a small decrease in DOM adsorption affinity at pH 5.5; the loss of components in the 3751–11350 Da fraction upon irradiation had little effect on adsorption because they played little or no role in the non-irradiated sample at this pH. Irradiation of DOM also affected its interactions with Fe in solution and the solution iron(II)/iron(III) speciation. The combined effects of irradiation followed by adsorption produced DOM that was lower in molecular weight and had a decreased UV-Vis absorptivity than either process, alone. Together, these two processes are likely to have important environmental consequences in terms of UV penetration of surface waters, contaminant mobility, and DOM bioavailability.

1. INTRODUCTION

Dissolved organic matter (DOM) strongly influences the fate and transport of pollutants such as trace metals (Lofts and Tipping, 2000; Tipping et al., 2002; de la Rosa et al., 2003) and hydrophobic organic compounds (HOCs) (Murphy et al., 1990), the attenuation of UV light in surface waters (Yan et al., 1996; Pullin and Cabaniss, 1997), and the rates and byproducts of photoreactions (Scully et al., 1995; Miller and Moran, 1997; Gao and Zepp, 1998; Zepp et al., 1998; Goldstone et al., 2002; Southworth and Voelker, 2003). The reactivity of DOM is influenced by its physicochemical characteristics such as molecular weight, aromaticity, and the presence and placement of reactive functional groups.

A wide array of environmental processes such as biodegradation (e.g., Kalbitz et al., 2003), coagulation (Benner and Opsahl, 2001; Maurice et al., 2002a), photodegradation (Gao and Zepp, 1998; Goldstone et al., 2002; Hernes and Benner, 2003a), and adsorption to mineral surfaces (e.g., Tipping, 1981; Davis, 1982; Gu et al., 1995; Zhou et al., 2001; Filius et al., 2003) have been shown to affect DOM concentrations and/or properties. In natural systems, these processes can occur sequentially or simultaneously, and may have additive or counteracting effects on the resulting DOM properties. For example, the combined effects of DOM photodegradation and biodegradation can be greater than the simple sum of the effects of the individual processes (Miller and Moran, 1997; Moran et al., 2000). The research described herein was designed to determine how photoirradiation affects DOM adsorption to the common Fe(III) oxyhydroxide mineral, goethite. Such a combination of processes might occur in nature, for example, at the confluence of a DOM-rich river with a sediment-laden river (e.g., McKnight et al. 1992) or during hyporheic exchange between river water and surrounding sediments (e.g., Maurice et al., 2002a).

Photoirradiation decreases the concentration of DOM (measured as dissolved organic carbon concentration, [DOC]), and degrades larger DOM components into smaller organic molecules (Mopper and Stahovec, 1986; Kieber and Mopper, 1987; Kieber et al., 1990; Wetzel et al., 1995; Moran and Zepp, 1997; Bertilsson and Travnik, 1998; Bertilsson and Bergh, 1999; Goldstone et al., 2002). Photoirradiation also decreases the UV- and visible light-absorbing properties of DOM (Bertilsson and Bergh, 1998; Gao and Zepp, 1998; Moran et al., 2000; Goldstone et al., 2002), a process that may lead to decreased attenuation of solar radiation in lakes (e.g., Morris et al., 1995; Morris and Hargreaves, 1997). Photoirradiation may also decrease the metal binding affinity of DOM through oxidation of the metal-binding carboxylic acid groups (Faust and Zepp, 1993; Gao and Zepp, 1998).

DOM adsorption to Fe(III)oxyhydroxides decreases with increasing pH (Tipping, 1981; Davis, 1982). The most important adsorption mechanism is ligand exchange (between DOM carboxylic acid and/or hydroxyl/phenolic groups and surface Fe), although other processes, such as hydrophobic interactions, may also be important (Tipping, 1981; Tipping and Cooke, 1982; Schulthess and Huang, 1991; Gu et al., 1994; Vermeer et al., 1998). DOM exhibits adsorption characteristics similar to those described for polydisperse polymers, including: rounded shape of isotherms, isotherms dependent upon sorbent surface-area-to-volume ratio, and adsorption-desorption hysteresis (Koopal, 1981; Vermeer et al., 1998; Zhou et al., 2001). Several groups have suggested that intermediate and/or high

* Author to whom correspondence should be addressed (pmaurice@nd.edu).
† *Present address:* Dept. of Chemistry, New Mexico Institute of Mining and Technology, Socorro, NM 87801 USA

molecular weight, more aromatic components of DOM adsorb preferentially to Fe(III)oxyhydroxide surfaces (Davis and Gloor, 1981; Tipping, 1981; McKnight et al., 1992; Gu et al., 1995; Kaiser and Zech, 1997; Meier et al., 1999; Namjesnik-Dejanovic et al., 2000; Zhou et al., 2001; Hur and Schlautman, 2003), leaving behind lower molecular weight, more aliphatic components in solution. This process has been termed 'sorptive fractionation.'

The purpose of this study was to determine the effect of prior photoirradiation on the sorptive fractionation process. Considering that DOM adsorption is preferential to high- to intermediate-MW components, that photoirradiation decreases the average molecular weight (MW) of DOM, and that photoirradiation could destroy the carboxyl groups responsible for surface binding, we hypothesized that photoirradiation would decrease the adsorption affinity of DOM for goethite. We tested this hypothesis by comparing the adsorption to goethite of photo-irradiated versus non-irradiated DOM at pH 3.5 and 5.5. In these experiments, Fe concentrations also were measured, because Fe-DOM interactions are important aspects of photochemical processes and potentially of adsorption.

2. MATERIAL AND METHODS

2.1. Basic Experimental Design

The basic experimental design for this study was as follows (details given below). An aqueous solution of a DOM isolate was irradiated in a solar simulator (vs a dark control). The irradiated and non-irradiated DOM solutions were then diluted to generate a range of dissolved organic carbon (DOC) concentrations for batch sorption experiments with goethite. Dissolved organic carbon analysis was used to measure the amount of DOM in solution before and following adsorption, and by difference the amount adsorbed. Size exclusion chromatography was used to measure the changes in molecular weight distributions of the DOM upon irradiation and adsorption. The concentrations of four low molecular weight carboxylic acids (known DOM photodegradation products) were measured after irradiation and adsorption. Dissolved total Fe and Fe(II) concentrations were also monitored.

2.2. Goethite Sample

Goethite was synthesized using the pure goethite method 5.2.1 of Schwertmann and Cornell (1991). X-ray diffraction analysis conducted using a Rigaku Miniflex powder X-ray diffractometer with a Cu X-ray tube showed goethite with no other detectable phases. BET surface area, measured with a model SA3100 volumetric sorption analyzer from Coulter Instruments, Inc. using N_2 adsorption at −195°C, was determined to be 51.5 $m^2\ g^{-1}$. For the adsorption experiment described below, a goethite stock suspension of 4.85 g L^{-1} was made in 0.2 μm filtered, ultraviolet light treated, deionized water (>17.8 mol/LΩ) (referred to as "deionized water" throughout), in a polypropylene bottle, and shaken on a platform shaker overnight in the dark, before the experiments.

2.3. Dissolved Organic Matter Sample

DOM-rich surface water was concentrated on-site on June 6, 2002 from Nelson's Creek, a first-order stream in the Ottawa National Forest (MI, USA), using a portable RealSoft PROS/IS reverse osmosis (RO) system (Serkiz and Perdue 1990; Sun et al. 1995). Concentration of DOM by RO allowed for sample storage, and for use in a wide range of other experiments and analyses not reported herein. A comparison by our group of photodegradation of bulk filtered water from Nelson's Creek versus XAD-8, XAD-4, and RO isolates has shown that the RO isolate closely mimics the photodegradation behavior of the bulk filtered water, perhaps because RO maintains the broad range of DOM components and the concentration of Fe, which plays an important role in photodegradation (Golden, Pullin, Maurice unpub. data). Operation of the RO system was similar to the procedure described by Serkiz and Perdue (1990), and included in-line treatment with Dowex-50 cation exchange resin (Na form) to decrease the calcium concentration before passing through the RO membrane, preventing membrane fouling due to the precipitation of $CaCO_3$. The final [DOC] of the retentate was 4.5 g C L^{-1}. The RO retentate was stored in amber glass bottles in refrigeration for 7 months, until the start of the experiment.

Table 1. Comparison of the physicochemical characteristics of Nelson's Creek filtered bulk water and diluted RO retentate.

Parameter	Filtered Bulk Water	Diluted RO Retentate
pH	5.52	5.5
conductivity (μS cm^{-1})	25.8	not measured
Fe (mg L^{-1})	0.394	0.284
Al (mg L^{-1})	0.306	0.218
Ca (mg L^{-1})	4.13	0.834
Mg (mg L^{-1})	1.12	0.273
Si (mg L^{-1})	1.64	1.24
Na (mg L^{-1})	0.261	1.34
K (mg L^{-1})	0.438	0.945
DOC (mg L^{-1})	28.0	33.8
DOM M_w (Da)	2092	2531
DOM M_n (Da)	1417	1593
DOM ρ (M_w/M_n)	1.48	1.59

Comparison of chemical analyses of Nelson's Creek bulk water (conducted shortly after sampling) and the stock solution of Nelson's Creek RO retentate (diluted with deionized water to 24 mgC L^{-1}) is provided in Table 1. This data set shows that the RO process resulted in a small increase in weight average molecular weight (M_w) and number average molecular weight (M_n) of the DOM retentate relative to the bulk water DOM. A similar effect was noted by Maurice et al. (2002b) on a stream-water sample from the New Jersey coastal plain and was attributed to possible condensation of the RO isolate during the isolation process.

2.4. Steady-State Adsorption Isotherms

Photodegradation and batch adsorption experiments were conducted at pH 3.5 and 5.5. For each pH, one liter of 27 mg C L^{-1} stock solution was made by diluting RO retentate with deionized water (>17.8 MΩ). The pH was adjusted to 3.5 or 5.5 using 0.1 mol L^{-1} NaOH and 0.1 mol L^{-1} HCl, after which the 1 L stock solution was split into two 500 mL volumes, one for irradiation and the other as a non-irradiated control. The non-irradiated control was stored in the dark at room temperature in a Parafilm M® covered glass beaker. The second 500 mL split was irradiated in an acid-washed and combusted (450°C, 12 h) 1 L jacketed beaker, through which cooled water was circulated to maintain a constant sample temperature of 18°C during the irradiation process. During irradiation, the solution was covered by Glad Cling Wrap® to prevent evaporation and contamination by airborne particles. Previous analysis of deionized water treated in the same manner showed that there was no measurable leaching of dissolved organic carbon from the wrap into the solution, and no contamination by UV-Vis light absorbing compounds (200–800 nm). The DOM sample was placed in a Suntest CPS+ solar simulator and irradiated for 48 h at a dosage of 750 W m^{-2}, ~2–3 times the intensity of noontime summer sunlight. The final collective irradiation dosage to a sample was 129600 kJ m^{-2}. A decrease (10–20%) in the intensity of the incident light across the solar spectrum occurred due to the Cling Wrap; however, the spectral distribution was unaltered (Progess, 2003), including light in the UV region.

Immediately following irradiation, batch-mode sorption experiments were conducted using the irradiated and non-irradiated water at both pH 3.5 and 5.5. The irradiated and non-irradiated stock solutions were diluted with deionized water to a range of concentrations. A final electrolyte concentration of 0.1 mol L^{-1} $NaClO_4$ was obtained in these solutions and also in DOM-free blanks by adding an appropriate amount of 1.0 mol L^{-1} $NaClO_4$ stock. Solution pH values were

adjusted to either 3.5 ± 0.1 or 5.5 ± 0.1 using 0.01 mol L^{-1} NaOH (99.99%, Aldrich) and/or 0.01 mol L^{-1} HCl (99.999%, Aldrich). Twenty-three mL of each dilution were added to 4 acid washed (10% HCl overnight) 28 mL polypropylene centrifuge tubes. 2 mL of the goethite stock was added to 3 of the 4 tubes for each dilution. before adding the goethite to the reaction vessels, the goethite stock suspension was ultrasonicated for ~10 s. Two mL of deionized water were added to the fourth tube to serve as a control. After the addition of goethite, the pH of each tube was readjusted to 3.5 or 5.5 (± 0.1), as needed. The samples were shaken for 24 h in the dark on a rotary shaker at room temperature (22°C). The pH values of the suspensions were measured following reaction and were found to be within ± 0.2 U. The samples were centrifuged at 13500 rpm for 17 min (Marathon 2100, Fisher) and filtered through precleaned (1.0 mol L^{-1} HCl followed by deionized water) 0.2 μm polyethersulfone syringe filters directly into glass vials for [DOC], UV/Vis absorbance, Fe(II), and HPSEC analysis, and polycarbonate test tubes for total Fe analysis. Samples for [DOC] analysis were acidified to pH ~2.0 by adding 10 μL 2.0 mol L^{-1} HCl (99.999%, Aldrich) for every 1 mL of sample. Samples for the analysis of total dissolved iron were also acidified to pH < 1 by adding 15 μL of concentrated HNO_3 (99.999%, Aldrich) to 5 mL of filtered sample. UV-Vis absorbance and iron(II) analyses were conducted immediately and the [DOC], HPSEC, and total dissolved iron analyses were conducted within two weeks. Time-consuming low molecular weight acid analysis was completed within 2 months. Samples were stored in dark refrigeration until analyzed.

No attempt was made to conduct desorption experiments. Previous work has shown that DOM sorption on goethite is highly irreversible (Gu et al., 1994; 1995). This was attributed to the formation of strong, multi-site surface complexes between the DOM and the goethite. However, it is also possible that some oxidation of the organic matter occurred at the goethite surface.

2.5. DOC, UV-Visible Spectrophotometry and Fe Analysis

[DOC] was analyzed on a Shimadzu TOC-5000 analyzer. The relative standard deviation (RSD) of 3–5 replicate injections was ≤ 2%. UV-visible absorbance spectra (200–800 nm) were collected on a Varian Cary 3 double-beam spectrophotometer, using 1.0 cm quartz cells. Samples were scanned from 600 to 200 nm at a rate of 100 nm/min. Molar absorptivity at 280 and 350 nm (on a DOC basis) has been shown to be linearly correlated with NMR-measured DOM aromaticity. The absorbance values at 280 nm and 350 nm and [DOC] were used to determine the DOM molar absorptivity at 280 and 350 nm (absorbance/DOC, with resulting units of L(mole C^{-1})(cm^{-1})).

Total dissolved (<0.2 μm) Fe concentrations were analyzed on a Perkin Elmer Optima inductively coupled plasma optical emission spectrometer (ICP-OES) at 238.204 nm, using external standards diluted from a NIST certified commercial stock. Fe(II) analysis was conducted using Ferrozine colorimetric analysis. Three mL of sample were mixed with 300 μL of a Ferrozine stock solution containing 10.0 mM Ferrozine (3-(2-pyridyl)_5,6-diphenyl-1,2,4-triazine-4′,4′′-disulfonic acid) and 1.0 mol L^{-1} hemisodium MES (2-(N-morpholino)ethanesulfonic acid). The MES buffers the reaction pH at 6.0, where the reduction of Fe(III) to Fe(II) by the Ferrozine itself does not occur (Pullin and Cabaniss, 2001). The absorbance of the resulting Fe(II)-Ferrozine complex was immediately read at 562 nm on a Varian Cary 3 double beam spectrometer, with deionized water as a reference. Standardization used solutions of ferrous ammonium sulfate hexahydrate in pH 2.0 nitric acid, made fresh daily. Analysis of Fe(II) was conducted within one hour of the completion of the irradiation and adsorption parts of the experiments, thus minimizing errors due to changes in the Fe(II) concentrations over time.

2.6. Determination of Molecular Weight Using HPSEC

High pressure size exclusion chromatography (HPSEC) was used to determine the average molecular weight of light-absorbing DOM before and after irradiation and adsorption (Chin et al., 1994, as modified by Zhou et al., 2000). The Waters HPSEC instrumentation included a Waters 2695 HPLC system, and a Waters 2996 photodiode array detector. The analysis used a Waters Protein-Pak 125 column. The mobile phase consisted of 0.10 mol L^{-1} NaCl buffered with 4 mM potassium phosphate at pH 6.8. The analysis was calibrated using a set of four random coil polystyrene sulfonate polymers (PSS; purchased from Polysciences, Inc., PA) dissolved in water to a concentration of 100 mg L^{-1} with peak molecular weights (M_p) = 15800, 6430, 4929, 1370 Da. Acetone (99.5% purity) and sodium salicylate (Fluka 99% purity) (M_p = 58 and 138 Da respectively) dissolved in deionized water (200 mg L^{-1}) were also used to calibrate the low end of the molecular weight distribution (Zhou et al., 2001). A linear regression between log peak molecular weight and retention time was used for calibration. Average cutoffs at 1% of the maximum intensity for high MW and at 2% of the maximum intensity for the low MW were used (see Cabaniss et al., 2000). The weight and number average molecular weights and the polydispersity (M_w, M_n, and ρ, respectively) of the DOM molecular weight distributions were calculated using the Waters Empower® GPC software package. Detailed definitions of these parameters and a discussion of DOM molecular weight distributions are given by Cabaniss et al. (2000).

While absorbance detection was simultaneously monitored at a variety of wavelengths using the PDA detector (200–450 nm), little difference in any of the molecular weight distributions over this wavelength range was observed. As a result, only the data from 254 nm detection are presented here. However, if an eluting substance does not absorb at this wavelength, its influence on the DOM molecular weight would be missed by our technique. Hereafter, molecular weight descriptions of DOM should be taken to mean the molecular weight of the components that absorb light at 254 nm wavelength.

2.7. Calculation of Molecular Weight Fraction Isotherms

The total molecular weight distribution (MWD) of each sample was divided into 6 different fractions based on molecular weight (50–150, 151–450, 451–1250, 1251–3750, 3571–11350, and 11351–18450 Da, as well as the summed total of the fractions). The area of the MWD taken up by each fraction was determined for each sample. The difference between the peak areas after adsorption and in the goethite-free controls (the "adsorbed peak area") was calculated for each fraction. To convert these adsorbed peak areas to adsorbed [DOC] (mg C m^{-2}), a linear regression between the adsorbed areas and the adsorbed [DOC] (mg C L^{-1}) from the DOC analysis was calculated for each fraction. Once converted to [DOC], the adsorbed [DOC] values were divided by the goethite surface area (in m^2 L^{-1}) to obtain the adsorbed [DOC] of each fraction in mg C m^{-2}. These values were plotted against equilibrium carbon concentration (C_{eq}) to obtain the isotherms of each MW fraction. In all cases (except the irradiated DOM at pH 3.5), the data had to be scaled so that the calculated total isotherm of all the fractions on a DOC basis approximated that of the isotherm determined using the bulk DOC data.

It is important to note that this methodology assumes that DOM molar absorptivity (at 254 nm) does not vary with molecular weight. However, previous work suggests that the higher molecular weight components of DOM have higher molar absorptivities (Chin et al., 1994; Namjesnik-Dejanovic et al., 2000). Thus, the approach used here may bias the data toward the higher molecular weight components of the DOM.

2.8. Low Molecular Weight Acid Analysis

Low molecular weight (LMW) carboxylic acids were measured by HPLC, as described in detail by Goldstone et al. (2002). Briefly, the LMW acids are derivatized to form relatively non-polar and chromophoric 2-nitrophenylhydrazines, which are then separated by reversed-phase HPLC with absorbance detection (400 nm) (Miwa et al. 1985; Mueller-Harvey and Parkes 1987; Albert and Martens 1997). The method gives baseline resolution of glycolic, lactic, formic, acetic, levulinic, malonic and oxalic acids in 35 min. Using 100 μL injections, the detection limit is 100 nM and the peak area response is linear to at least 100 μmol L^{-1}. Glycolic, lactic and levulinic acids were not observed above background in any of our samples.

Table 2. Effects of irradiation on [DOC] and DOM properties at pH 3.5 and 5.5

Sample	[DOC] (mg C L^{-1})	ε_{280} (L $molC^{-1}$ cm^{-1})	ε_{350} ($LmolC^{-1}$ cm^{-1})	M_w (Da)	M_n (Da)	ρ
pH 3.5						
non-irradiated	27.4	323	116	2259	1446	1.56
irradiated	22.9	250	73.3	1209	771	1.55
pH 5.5						
non-irradiated	33.8	501	189	2531	1593	1.59
irradiated	31.2	423	144	1197	791	1.51

3. RESULTS

3.1. Effects of Irradiation on DOM Characteristics

At pH 3.5, [DOC] decreased by ~16% upon irradiation, and at pH 5.5 by ~8% (Table 2). Irradiation also substantially decreased the molar absorptivity of the DOM (Table 2). This change was not equal over the entire UV-Vis wavelength range observed here (200–800 nm). The maximum relative loss in molar absorptivity due to irradiation was centered at 350 nm (Progess 2003), so that ε_{350} was followed during sorption. Additionally, Traina et al. (1990) and Peuravuori and Pihlaja (1997) have described ε_{280} as being linearly proportional to the NMR-measured aromaticity of DOM, so that ε_{280} also was followed during sorption (data discussed below).

The peak MW of non-irradiated DOM decreased slightly at pH 3.5 when compared to pH 5.5 (Table 2, Fig. 1). The peak MW decreased substantially upon irradiation at both pH 3.5 and 5.5 (Table 2, Fig. 1). At both pH values, irradiation decreased the abundance of higher molecular weight components, increased the abundance of low molecular weight components, and shifted the peak molecular weight to a lower value. As a result, average molecular weight (both M_w and M_n) decreased by about half upon irradiation at both pH values (Table 2).

Low (but measurable) concentrations of acetic, formic, and oxalic acids were noted in the non-irradiated samples (Fig. 2, Table 3). The concentrations of formic, malonic, and acetic acids increased substantially upon irradiation at both pH values, and the increases were slightly greater at pH 5.5 than at pH 3.5 (Table 3). Formic acid was produced in the highest concentration at both pH values, followed by acetic and malonic acids (Table 3). At pH 5.5, we also observed a slight net increase in oxalic acid due to irradiation, although no net increase was detected at pH 3.5 (Table 3).

3.2. Effects of Irradiation on Adsorption

3.2.1. Adsorption isotherms

Adsorption isotherms for the non-irradiated and irradiated DOM at pH 3.5 are shown in Figure 3a. At pH 3.5, DOM adsorption did not attain a clear plateau over the range of concentrations studied herein. However, the greatest observed adsorption density was up to ~2 times larger for non-irradiated than irradiated samples, 0.37 ± 0.03 vs. 0.17 ± 0.03 (in mg C m^{-2}, ± 1σ, n = 3). The adsorption isotherms for non-irradiated and irradiated DOM at pH 5.5 are shown in Figure 3b. While the differences in the maximum adsorption density between the non-irradiated (0.18 ± 0.02 mg C m^{-2}) and irradiated DOM (0.15 ± 0.01 mg C m^{-2}) were smaller at pH 5.5 (determined as the average of the highest five values, ± 1σ), their difference was still statistically significant at the 95% confidence level (t-test). In agreement with results of previous studies (e.g.,

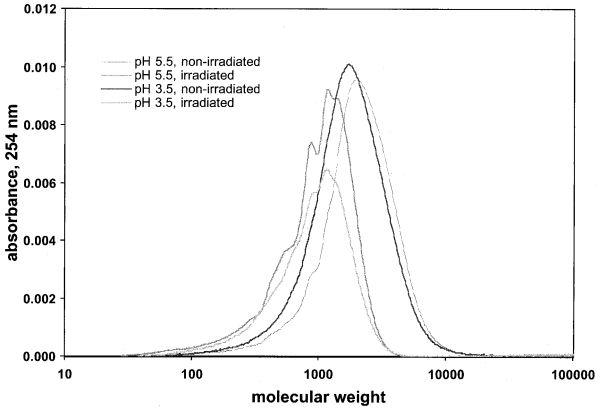

Fig. 1. The effect of irradiation on DOM molecular weight distributions at pH 3.5 and 5.5. At both pH values, irradiation results in a loss of high molecular weight components and a gain of low molecular weight components, resulting in a substantial decrease in average molecular weight.

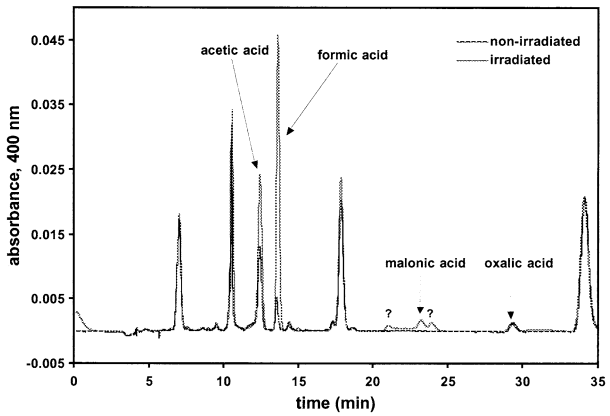

Fig. 2. Representative LMW acid chromatograms show the effects of irradiation on the concentrations of several LMW acids at pH 3.5. Chromatograms are for the separation of the 2-nitrophenylhydrazide derivatives of the LMW acids (see Methods for details). Known LMW acid peaks are labeled with their identities, peaks of unknown LMW acids are labeled as "?"; all other peaks are byproducts of the derivatization reaction.

Table 3. Effect of irradiation on the concentrations of four low molecular weight carboxylic acids.

Sample	Acetic (μmol L^{-1})	Formic (μmol L^{-1})	Malonic (μmol L^{-1})	Oxalic (μmol L^{-1})
pH 3.5				
Non-irradiated	2.18 ± 0.02	0.622 ± 0.006	bdl[b]	2.5 ± 0.1
irradiated	16.2 ± 0.2	42.7 ± 0.4	13.1 ± 0.5	2.4 ± 0.1
pH 5.5				
Non-irradiated	0.931 ± 0.009[a]	0.344 ± 0.003	bdl	1.38 ± 0.07
irradiated	14.8 ± 0.2	41.2 ± 0.4	15.8 ± 0.6	3.4 ± 0.2

[a] errors are ±1 standard deviation.
[b] bdl = below detection limit of 0.3 μmol L^{-1}.

Tipping, 1981; Gu et al., 1994, 1995; Zhou et al., 2001; Namjesnik-Dejanovic et al., 2000), we observed that adsorption of non-irradiated DOM to goethite increased with decreasing pH from 5.5 to 3.5. However, in the case of the irradiated DOM, the difference between the maximum adsorption density at pH 5.5 and the greatest observed adsorption at pH 3.5 was much smaller, only statistically significant at the 80% confidence level (t-test). Because adsorption did not reach its maximum value at pH 3.5 in our experiments, this difference might be underestimated by our data. In any case, after irradiation, the effect of pH on DOM adsorption to goethite is much smaller.

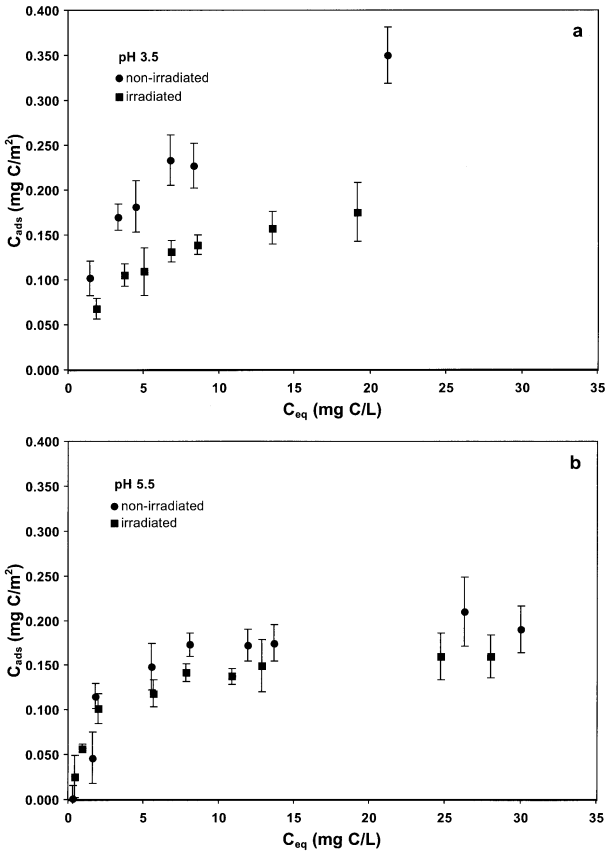

Fig. 3. The effect of irradiation on the overall adsorption of DOM on goethite at (a) pH 3.5 and (b) pH 5.5. Values are the average of 3 separate experiments, ±1 standard deviation. Equilibrium adsorbed concentrations (C_{ads}) are normalized to goethite surface area.

3.2.2. *Molecular weight*

The effects of irradiation and adsorption on the molecular weight distributions (MWD) of irradiated and non-irradiated DOM at several DOM concentrations at pH 3.5 are shown in Table 4 and Figure 4. At low initial concentrations, corresponding to low surface coverage, all large and intermediate molecular-weight components were adsorbed, leaving only relatively small molecules in solution. At high initial DOM concentrations, corresponding to high surface coverage (a small percentage of the DOM adsorbed), a greater proportion of low to intermediate molecular-weight components remained in solution. Additionally, under these conditions, a small amount of the highest molecular weight fraction of the DOM mixture remained in solution. Adsorption of irradiated DOM at high surface coverages was preferential to high to intermediate molecular weight components. The highest molecular weight fraction in the original sample had been removed by irradiation, but the remaining highest molecular weight components were still preferentially adsorbed.

At pH 5.5 (Table 4 and Fig. 5), adsorption of non-irradiated DOM was preferential to intermediate molecular weight components, with little adsorption of either the highest or lowest molecular-weight fractions. This is especially apparent at low surface coverage (high relative sorption), where the DOM left in solution following sorption has a bimodal distribution (Fig. 5). The highest molecular-weight components that did not sorb at pH 5.5 were removed by photo-irradiation.

3.2.3. LMW acid adsorption

As noted earlier, LMW acids were measured in both the non-irradiated and irradiated samples. However, with the exception of oxalic acid, little to no adsorption of these compounds was observed in either sample type at either pH value. Oxalic acid showed a clear decrease in concentration upon reaction with goethite under all experimental conditions. However, the relative adsorption of oxalate to the surface varied from 0 to 62% for pH 3.5, nonirradiated; from 12 to 51% for pH 3.5, irradiated; from 0 to 70% for pH 5.5, nonirradiated; and from 0 to 64% for pH 5.5, irradiated, and did not show any consistent trend with either its concentration or the concentration of the DOM (data in Progess, 2003).

Table 4. Effect of irradiation and sorption on the DOM molecular weight distribution. "High sorption density" represents the highest C_{eq} in Figures 3a and 3b and "Low sorption density" represents the 2nd lowest C_{eq} in Figures 3a and 3b.

	% of total molecular weight distribution within the range (in Daltons)					
Sample	50–150	151–450	451–1250	1251–3750	3751–11,350	11,351–18,450
pH 3.5, non-irradiated						
Control	0.4%	3.1%	19.9%	60.9%	15.2%	0.4%
High sorption density	0.6%	4.1%	25.2%	58.2%	11.5%	0.4%
Low sorption density	0.0%	13.8%	61.8%	24.3%	0.0%	0.0%
pH 3.5, irradiated						
Control	1.9%	11.0%	44.8%	41.7%	0.7%	0.0%
High sorption density	2.8%	15.8%	53.9%	27.4%	0.1%	0.0%
Low sorption density	2.8%	32.4%	61.9%	2.9%	0.0%	0.0%
pH 5.5, non-irradiated						
Control	0.4%	2.3%	15.3%	64.9%	16.9%	0.3%
High sorption density	0.4%	2.6%	17.3%	60.4%	19.0%	0.4%
Low sorption density	4.5%	21.0%	47.6%	26.9%	0.0%	0.0%
pH 5.5, irradiated						
Control	2.2%	9.5%	45.5%	42.4%	0.2%	0.0%
High sorption density	2.4%	11.2%	52.2%	34.0%	0.1%	0.0%
Low sorption density	1.7%	17.4%	68.9%	12.1%	0.0%	0.0%

3.2.4. *Molar absorptivity*

During the adsorption of the irradiated and non-irradiated DOM to goethite at both pH 3.5 and 5.5, substantial decreases in the molar absorptivity (ε_{280} and ε_{350}) of the DOM remaining in solution were observed. As a result, the relative loss of absorbance upon sorption was larger than the relative loss of DOC upon sorption (Fig. 6). This indicates the preferential sorption of DOM moieties that absorb light at these wavelengths. If sorption were not preferential for the light absorbing fraction of the DOM, then the data would fall on the 1:1 line in the plots. It is important to note that these results are the net result of the adsorption process; some of the adsorbed molecules could have been weakly light absorbing.

3.3. Effects of Irradiation and Adsorption on Fe Speciation

Figures 7 and 8 show the effects of irradiation and adsorption on the total dissolved Fe concentration and the dissolved Fe(II) concentration at pH 3.5 and 5.5 (<0.2 μm). At pH 3.5, ~75%

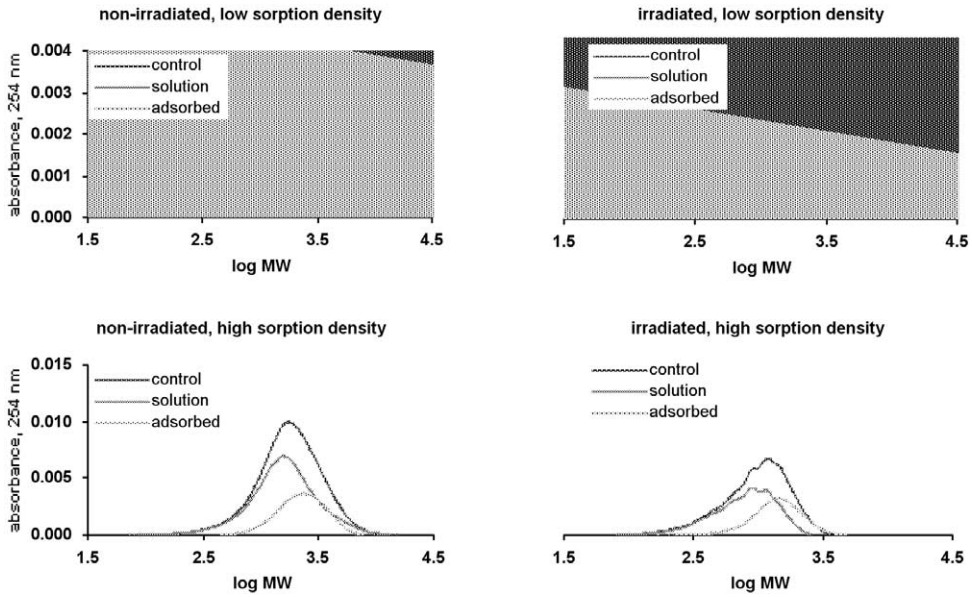

Fig. 4. Change in DOM molecular weight distributions upon irradiation and adsorption at pH 3.5. Top two figures are at low surface coverage (2nd smallest C_{eq} in Fig. 3, bottom two figures are at higher surface coverage (largest C_{eq} in Fig. 3). Figures on the left show effects of adsorption on molecular weight distributions of non-irradiated DOM. Figures on the right show effects of adsorption on molecular weight distributions of irradiated DOM. Control (no goethite) and solution (DOM remaining in solution after adsorption) molecular weight distributions are measured. Adsorbed molecular weight distributions are calculated by difference.

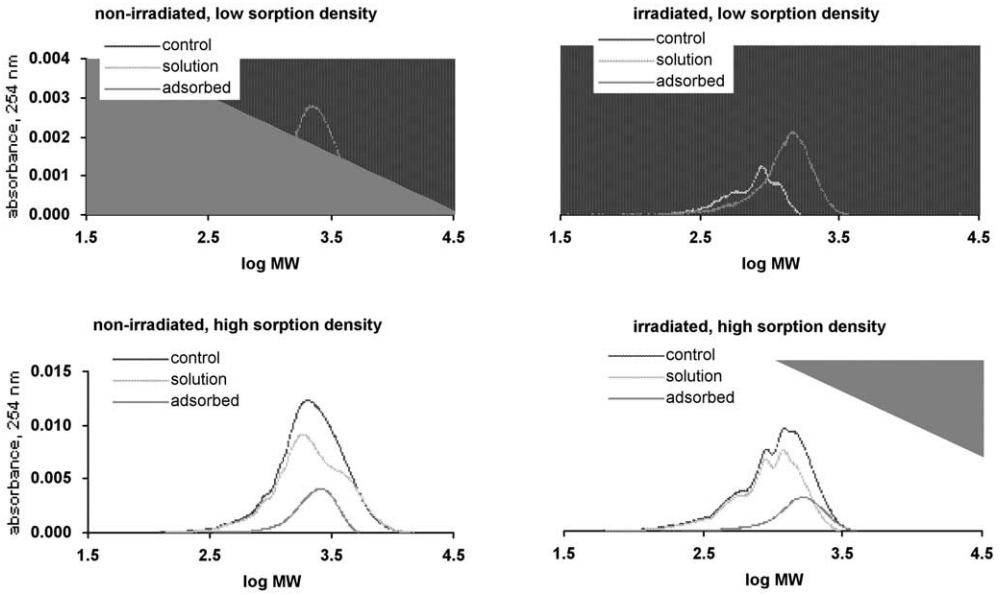

Fig. 5. Change in DOM molecular weight distributions upon irradiation and adsorption at pH 5.5. Top two figures are at low surface coverage (2nd smallest C_{eq} in Fig. 4), bottom two figures are at higher surface coverage (largest C_{eq} in Fig. 4). Figures on the left show effects of adsorption on molecular weight distributions of non-irradiated DOM. Figures on the right show effects of adsorption on molecular weight distributions of irradiated DOM. Control (no goethite) and solution (DOM remaining in solution after adsorption) molecular weight distributions are measured. Adsorbed molecular weight distributions are calculated by difference.

of the total iron was initially present as Fe(II) (Fig. 7a). After irradiation, this fraction increased to near 100% (Fig. 7b). At pH 5.5, only ~20% of the total iron was present as Fe(II), before irradiation (Fig. 8a). After irradiation, Fe(II) increased to ~50% of the total Fe (Fig. 8b).

At pH 3.5, the total Fe concentration increased over the course of the adsorption experiments using non-irradiated and irradiated DOM. In the non-irradiated sample, this increase was mainly caused by additional Fe(III) (Fig. 7a). However, in the irradiated sample, the increase was due to additional Fe(II) (Fig. 7b). At pH 5.5, total iron increased slightly during the sorption experiment using non-irradiated DOM (Fig. 8a). This occurred despite an observed decrease in Fe(II) during the same experiment. When the irradiated DOM was used at pH 5.5, a substantial decrease in iron (mostly as Fe(II)) was observed (Fig. 8b). There was no measurable iron in the non-DOM-containing controls reacted with goethite at both pH 3.5 and 5.5.

4. DISCUSSION

4.1. Effects of Irradiation on DOM Characteristics

Our results (Fig. 1, Tables 2 and 3) are consistent with those of a number of researchers (e.g., Gao and Zepp, 1998; Bertilsson and Bergh, 1999) who demonstrated that exposure of DOM to solar radiation results in the formation of lower molecular weight photoproducts and dissolved inorganic carbon (DIC), with a consequent decrease in the average molecular mass (e.g., Moran and Zepp 1997; Gao and Zepp, 1998; Bertilsson and Bergh, 1999; Maurice et al., 2002a). The HPSEC molecular weight distributions shown in Figure 1 confirm that irradiation results in removal of higher molecular weight DOM components, along with formation of new lower molecular weight components at both pH 3.5 and 5.5. This process results in an approximately 50% decrease in the peak and average DOM MW, with similar changes observed at both pH values (Table 2). Moreover, the decrease in peak height and peak area at both pH values indicates an overall loss of light-adsorbing DOM (at the detecting wavelength, 254 nm). Bertilsson and Bergh (1999) observed a 33% decrease in M_w and a 29% decrease in M_n of a stream fulvic acid at pH ~6 upon irradiation for 20 h using a variety of set-wavelength UV lamps. The greater decrease that we observed could be due to the longer exposure time, to the original DOM sample composition, and/or to differences in the wavelengths of light used for the irradiation experiments. A larger decrease in [DOC] during irradiation was noted at pH 3.5 than at pH 5.5 (Table 2). This may be the result of some precipitation at the lower pH, or higher efficiencies of iron photoreactions (due to its increased solubility).

It has been shown that the exposure of natural waters to sunlight produces LMW organic compounds such as carboxylic acids, aldehydes and ketones (Kieber et al., 1990; Goldstone et al., 2002). These LMW compounds are smaller, more biologically labile, and less light absorbing than DOM (Kieber and Mopper, 1987; Kieber et al., 1990; Moran and Zepp, 1997). Bertilsson and Tranvik (1998) showed that four LMW acids (acetic, formic, malonic, and oxalic) are formed at rates that are at least an order of magnitude higher than any other previously identified LMW organic photoproducts, and thus these compounds were measured herein.

We found significant increases in the concentrations of these four acids due to irradiation. Consistent with the work of Bertilsson and coworkers (Bertilsson and Tranvik, 1998, 2000; Bertilsson and Bergh 1999), we found that production of low

molecular weight organic acids during irradiation decreased in the order formic > acetic > malonic > oxalic. However, it is important to note that these LMW acid measurements represent the net result of the photoirradiation process. In addition to generating LMW acids, photochemical reactions can also destroy them. Generally, LMW carboxylic acids do not absorb light in the sunlight spectrum and therefore do not undergo direct photochemical decomposition. However, indirect photochemical processes can affect LMW acids. For example, formic acid can be consumed by hydroxyl radical, a byproduct of several photochemical processes (Goldstone et al., 2002). Additionally, oxalic acid can form a highly photoreactive solution complex with Fe(III), which decomposes to CO_2 and Fe(II) upon irradiation (Faust and Zepp, 1993; Bertilsson and Tranvik, 1998). Malonic acid also forms such a complex with Fe(III), although the efficiency of its photoreaction is several orders of magnitude smaller than that of the Fe(III)-oxalate complex (Faust and Zepp, 1993). In our experiments, the iron concentrations (~0.3 mg L^{-1}) were relatively high compared to the natural waters in which LMW acids were previously studied (Bertilsson and Tranvik, 2000) and this may explain why relatively little net oxalic acid formation was observed, despite previous reports of its photoproduction (Bertilsson and Tranvik, 1998, 2000).

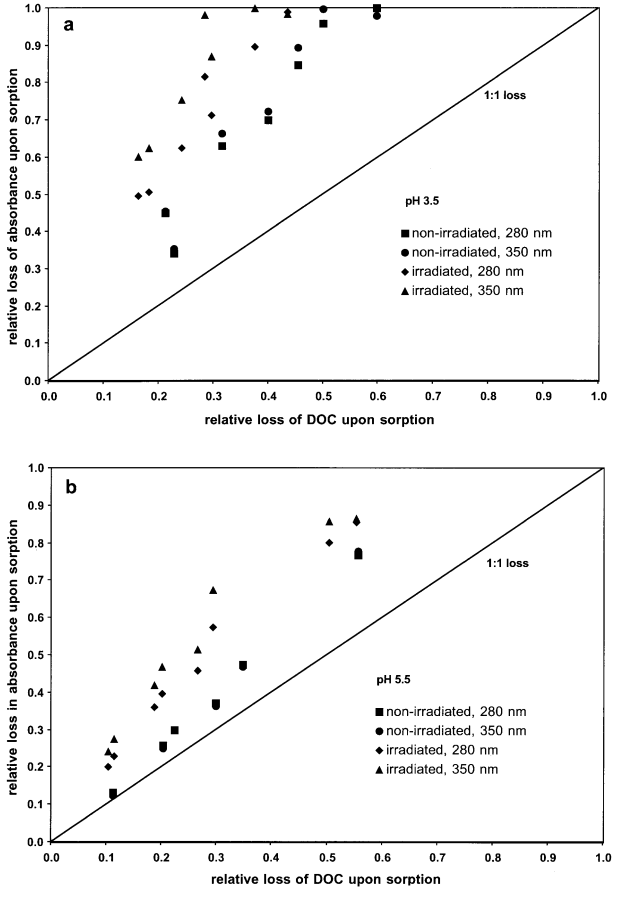

Fig. 6. Effect of sorption on DOM molar absorptivity at (a) pH 3.5 and (b) pH 5.5. The 1:1 loss line indicates the expected relationship between the parameters if no preferential sorption occurred.

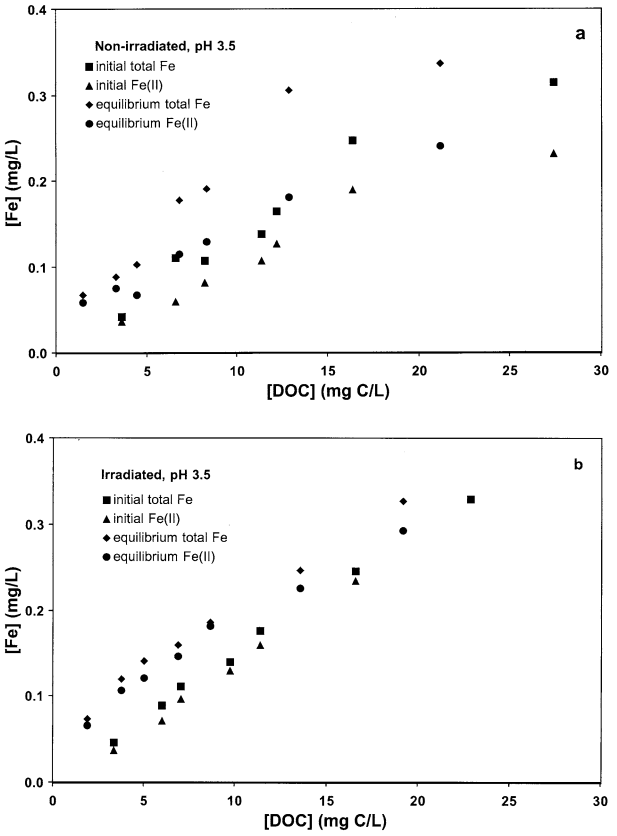

Fig. 7. Comparison of total Fe and Fe(II) concentrations in solution before (initial) and following (equilibrium) adsorption on goethite for (a) non-irradiated and (b) irradiated DOM at pH 3.5. Note that for the "initial" data, the x-axis data represent the [DOC] before exposure to goethite. For the "equilibrium" data, the x-axis represents the equilibrium [DOC] during adsorption or C_{eq}.

4.2. Effects of Irradiation on Adsorption

4.2.1. Adsorption isotherms

Davis and Gloor (1991) used gel exclusion chromatography to compare adsorption of different MW fractions (MW < 500, 4000–500, > 4000 Da) to aluminum oxide. They observed that the intermediate molecular weight fraction adsorbed most strongly. Zhou et al. (2001) used HPSEC to compare the contributions of six different MW fractions (10–150, 151–450, 451–1250, 1251–3750, 3751–11350, 11351–18450 Da) of a fulvic acid (M_w ~2200) to adsorption on goethite at pH 3.5, 5.5, and 7.5. They found that at all 3 pH values, the intermediate molecular weight fraction, 1251–3750 Da, dominated adsorption, and that the importance of larger DOM components to overall adsorption decreased from pH 3.5 to pH 5.5 and 7.5. This strong affect of pH on the adsorption of the highest molecular weight fraction of DOM may be due to its relatively high charge density. de Laat et al. (1995) and de Laat and van den Heuval (1995), who studied anionic polymers, suggested that greater charge on larger organic molecules may present an electrostatic barrier to adsorption, when in competition with smaller and less charged polymers, and at high surface coverage where closer proximity of adsorbing molecules would

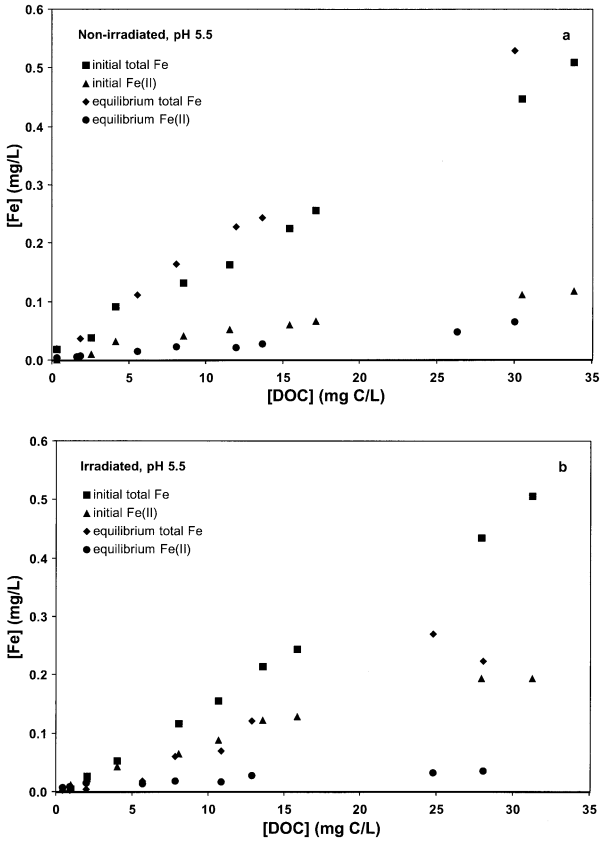

Fig. 8. Comparison of total Fe and Fe(II) concentrations in solution before (initial) and following (equilibrium) adsorption on goethite for (a) non-irradiated and (b) irradiated DOM at pH 5.5. Note that for the "initial" data, the x-axis data represent the [DOC] before exposure to goethite. For the "equilibrium" data, the x-axis represents the equilibrium [DOC] during adsorption or C_{eq}.

promote intermolecular repulsion. At the lower pH, anionic functional groups would tend to be more protonated, molecules more likely to be neutral, and hydrophobic interactions between more aromatic, higher molecular-weight components of neighboring molecules could stabilize their adsorption. At pH 5.5, more of the carboxyl groups would be deprotonated, and electrostatic repulsion between neighboring charged molecules would present a barrier to adsorption, particularly for the higher molecular-weight components.

To compare the contributions of different molecular weight components to adsorption, the MWD of the non-irradiated and irradiated DOM at pH 3.5 and 5.5 were each split into 6 MW fractions, (50–150 Da, 151–450 Da, 451–1250 Da, 1251–3750 Da, 3751–11350 Da, and 11351–18450 Da), as in Zhou et al. (2001). The resulting adsorption isotherms for each fraction are presented in Figures 9 and 10. At both pH values, adsorption of the non-irradiated DOM was dominated by the intermediate molecular weight 1251–3750 Da fraction (Figs. 9a and 10a). At pH 3.5, there were additional substantial inputs from the somewhat lower (151–140 Da) and somewhat higher (3751–11350 Da) molecular-weight fractions. Most of the decrease in adsorption from pH 3.5 to pH 5.5 was due to decreased adsorption of the 1251–3750 Da fraction, with additional decreases in the adsorption of the 451–1250 and 3751–11350 Da fractions. The very highest and lowest molecular weight fractions (50–150 Da and 11351–18450, respectively) played little to no role in adsorption at either pH. Our results confirm that the very highest MW components of the non-irradiated DOM; i.e., those with MW > ~3750, have lesser adsorption affinities for goethite at pH 3.5 and 5.5 than the more intermediate molecular weight components. At pH 5.5, only the intermediate MW components adsorb.

For irradiated DOM, at both pH values, the 1251–3750 Da fraction again controlled overall adsorption. The higher molecular weight components (>3750 Da, or >log MW ~3.5) were virtually non-existent in the photo-irradiated samples (Figs. 9b and 10b) and therefore contributed little or nothing to overall adsorption. The loss of higher molecular weight components upon irradiation did not substantially affect the overall adsorption at pH 5.5 because the higher molecular weight components did not adsorb in the non-irradiated sample. Thus, the molecular weight distributions of adsorbing components were very similar for the irradiated versus non-irradiated samples at pH 5.5 (Fig. 5).

However, since the high (>3750) molecular weight fraction did contribute to overall adsorption at pH 3.5, its loss during

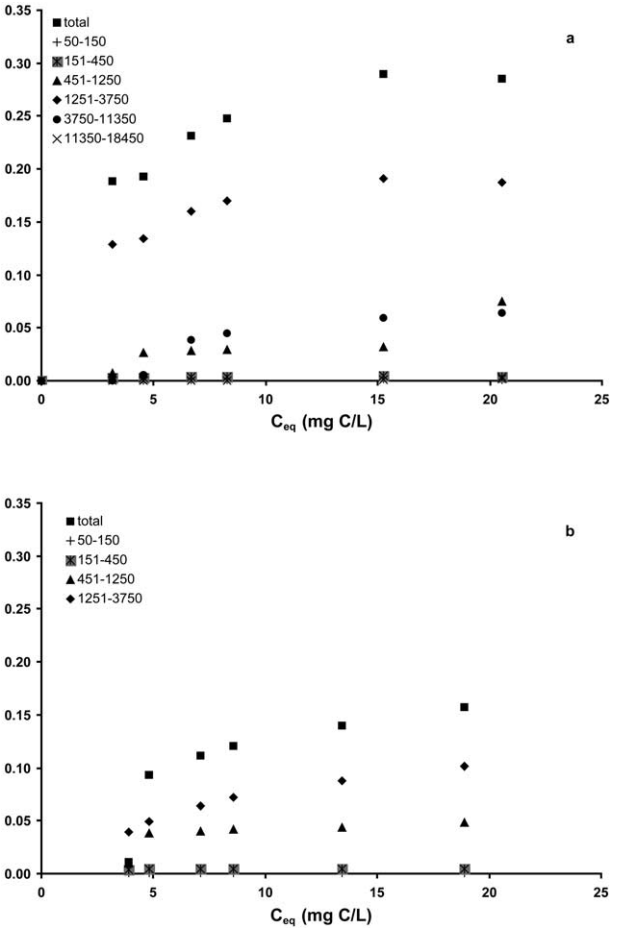

Fig. 9. Adsorption isotherms for various molecular weight fractions for (a) non-irradiated and (b) irradiated samples at pH 3.5. The two largest molecular weight fractions are not plotted in (b) because they were destroyed during the sunlight irradiation.

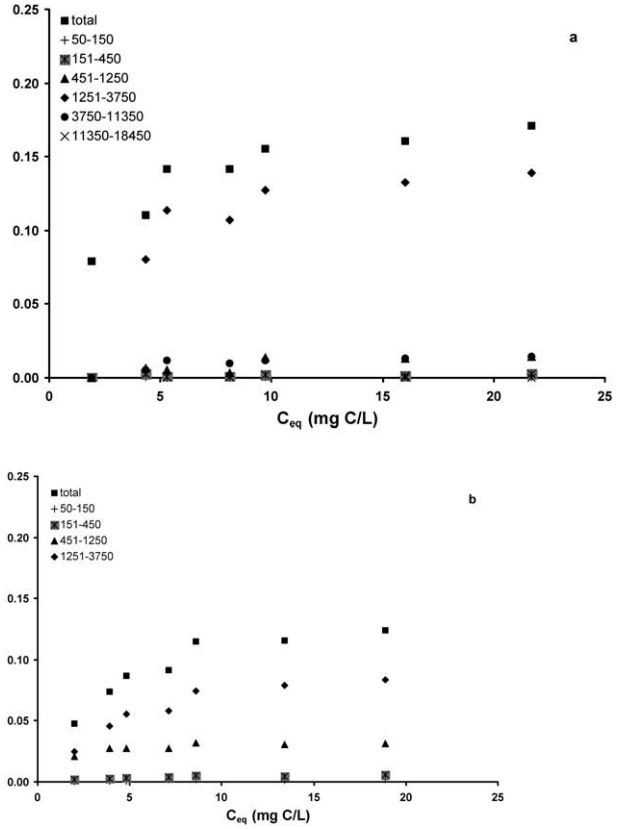

Fig. 10. Adsorption isotherms for various molecular weight fractions for (a) non-irradiated and (b) irradiated samples at pH 5.5. The two largest molecular weight fractions are not plotted in (b) because they were destroyed during the sunlight irradiation.

irradiation did decrease overall adsorption at pH 3.5 following irradiation. This result is consistent with the theory of de Laat and the conclusions reached in Zhou et al. (2001), that the high charge density of the higher molecular weight material presents a barrier to adsorption as pH increases.

In addition to the loss of the high molecular weight components, irradiation also caused a decrease in the adsorption of the intermediate molecular weight components (1251–3750 Da), especially at pH 3.5 (Fig. 9). This decrease could be due to complete removal (photo-oxidation) of the carbon in this weight range, but it could also be due to a decrease in the adsorption affinity of this material. Decreases in metal complexing ability (and thus adsorption affinity) might be caused by decreases in ionizable functional groups, such as light- and iron-mediated decarboxylation (Faust and Zepp, 1993; Gao and Zepp, 1998).

4.2.2. Molecular weight

Figure 11 shows the combined effects of irradiation and adsorption on the molecular weight of the DOM. The horizontal lines represent the average molecular weight (M_w) of the DOM before and after irradiation. The points show the additional effect of the adsorption process on the M_w. before irradiation, adsorption substantially decreases the DOM M_w. Although this effect is somewhat smaller in magnitude after irradiation, a substantial decrease in DOM M_w still occurs following adsorption. These results demonstrate that irradiation and adsorption act in concert to decrease the overall molecular weight distribution of DOM.

4.2.3. LMW acid adsorption

All four LMW acids examined here have been previously observed to undergo adsorption on goethite (Sigg and Stumm, 1981; Stumm and Sulzberger, 1992; Goldberg et al., 1993; Pehkonen et al., 1993; Horanyi, 2002; Wijnja and Schulthess, 2002). Therefore, the lack of significant adsorption of acetic, formic, and malonic acids, especially at relatively low concentrations where percent adsorption even in weakly adsorbing single-acid systems would be maximized, can perhaps be attributed to the competition for surface sites by the DOM. However, further study on competitive adsorption is needed.

In contrast, oxalic acid was able to compete successfully

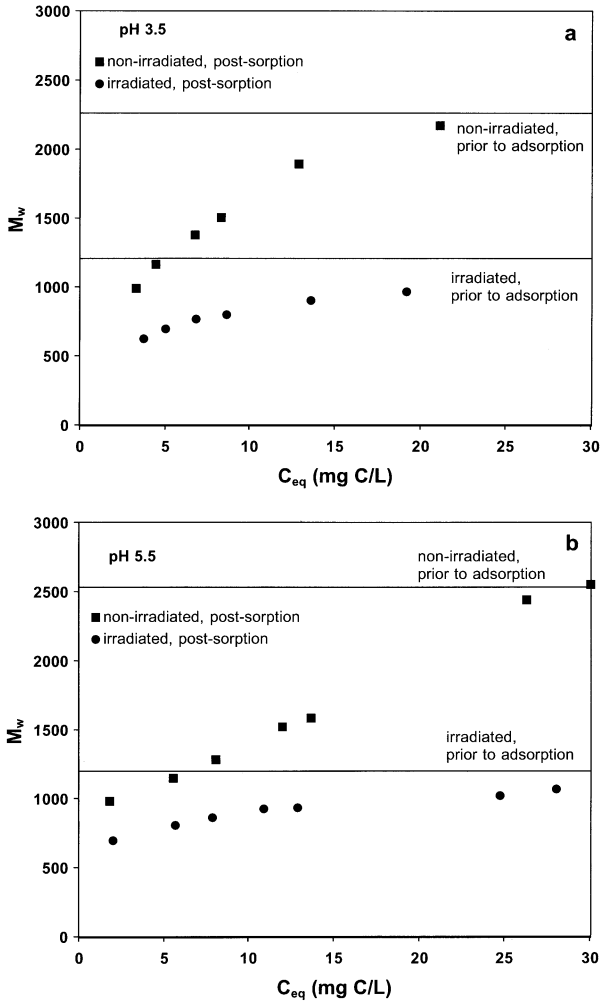

Fig. 11. Change in average molecular weight (M_w) of DOM remaining in solution following adsorption and irradiation. The M_w of DOM remaining in solution converges on initial (irradiated or non-irradiated) values at higher equilibrium concentrations because as surface coverage increases, a higher percentage of DOM remains in solution and the sorptive fraction becomes less important. (a) pH 3.5 (b) pH 5.5.

with DOM for surface sites, even at its fairly low concentrations. This may be due to its relatively strong affinity for Fe oxyhydroxide surfaces, as evidenced by its ability to form a bidentate mononuclear inner-sphere surface complex with goethite (Stumm and Sulzberger, 1992 and references therein). The fact that oxalic acid adsorption did not show any consistent trends may be due to the fact that both adsorbates (oxalate and DOM) varied simultaneously in concentration in the same direction. Additionally, the observed values of oxalic acid are near our instrumental detection limit, causing the data to be imprecise or noisy.

4.2.4. Molar absorptivity

The molar absorptivity of DOM at various UV wavelengths including 205, 254, 272 and 280 nm has been shown to correlate with ^{13}C-NMR-measured aromaticity (% of total carbon contained in aromatic subgroups) (Traina et al. 1990; Novak et al., 1992; Chin et al., 1994; Peuravuori and Pihlaja, 1997; Weishaar et al., 2003). This correlation is strongest when samples from similar organic matter sources and operational fractions are used, such as humic acids ($r^2 = 0.88$, n = 11; Traina et al., 1990), or aquatic fulvic acids ($r^2 = 0.97$, n = 13; Weishaar et al., 2003). When a more diverse set of organic matter samples are included in the correlation, such as whole water samples plus aqueous humic substances collected using a variety of techniques ($r^2 = 0.84$, n = 39; Peuravuori and Pihlaja, 1997) or soil humic acids, water-only soil extracts, and aquatic fulvic acids ($r^2 = 0.36–0.45$, n = 18; Novak et al. 1992), the relationship can be less significant.

In this study, the DOM molar absorptivity at 280 nm (ε_{280}) decreased during irradiation by ~75 U at both pH 3.5 and 5.5, suggesting that irradiation was selective for the aromatic components of DOM (Table 2). Additionally, for both non-irradiated and irradiated samples, adsorption markedly decreased the ε_{280} of DOM remaining in solution following adsorption, especially at low equilibrium [DOC] (Fig. 6). This suggests preferential adsorption of aromatic-containing moieties from the DOM mixture. Similar results have been observed previously for non-irradiated DOM adsorption to Fe(III) oxyhydroxides and clays (Meier et al., 1999; Namjesnik-Dejanovic et al. 2000; Maurice et al., 2002a). This large decrease in ε_{280} indicates that the DOM remaining in solution after photodegradation and adsorptive fractionation is less aromatic than the starting material. Our results also demonstrate that the combined effect of irradiation and adsorption on solution aromaticity is considerably greater then the effects of either irradiation or adsorption, alone.

Recently, Hernes and Benner (2003b) noted a strong positive, linear correlation between absorbance at 350 nm and the concentration of lignin phenols (aromatic moieties in terrestrially-derived organic matter). Furthermore, this relationship was unaffected by the molecular size of the DOM used for the absorbance measurements. This suggests that absorbance at 350 nm is also a good indicator of the lignin and/or aromatic content of DOM. Thus, our observation of the selective adsorption of DOM with high ε_{350} also suggests preferential sorption of lignin-derived aromatic moieties within the DOM mixture.

It is important to note that the correlation between aromaticity and UV molar absorptivity has not been tested for changes in the chemical structure of a single sample (although natural surface water samples often have undergone some degree of photo-irradiation or sorptive fractionation in the field). Certainly, it is possible that DOM contains non-aromatic structures that also absorb at 280 nm and that these structures could undergo photochemical transformation or preferential sorption. However, our interpretation of the data presented here is supported by the results of McKnight et al. (1992) who directly observed the preferential sorption of aromatic moieties on iron oxides in a field setting using ^{13}C-NMR.

4.3. Effects of Irradiation and Adsorption on Fe Speciation

4.3.1. Irradiation

At pH 3.5, the majority of the iron is present as Fe(II), both before and after irradiation (Fig. 7). This is due to a net thermal (or "dark") reduction of Fe(III) to Fe(II) by reducing moieties on the DOM, possibly reduced quinone or catechol-type structures (Scott et al. 1998; Pullin and Cabaniss 2003a). At this pH, the rate of this process is relatively fast (Voelker and Sulzberger, 1997) and the rates of Fe(II) oxidation by O_2 and H_2O_2 are very slow (Sung and Morgan, 1980), leading to the conversion of the majority of the iron to Fe(II).

The concentration of iron initially present as Fe(II) at pH 5.5 (Fig. 8) is smaller than at pH 3.5, consistent with slower rates of thermal reduction and faster rates of oxidation at this pH value (Sung and Morgan, 1980; Voelker and Sulzberger, 1996; Voelker et al. 1997; Pullin and Cabaniss, 2003a; 2003b). Upon irradiation, the amount of Fe(II) (relative to total iron) increases. Previous researchers have shown that Fe(III) can be photoreduced to Fe(II) in the presence of DOM (e.g., Faust and Zepp, 1993; Kieber at al, 2003).

4.3.2. Adsorption

Following the reaction of non-irradiated and irradiated DOM with goethite at pH 3.5, the net concentrations of total Fe and Fe(II) increased (Fig. 7), indicating that the DOM caused net dissolution of the goethite (no dissolution was seen in DOM-free controls). In the non-irradiated sample, this dissolution resulted mainly in increased concentrations of Fe(III), suggesting ligand-promoted dissolution by the DOM. Many previous investigators have observed ligand-promoted Fe(III)oxhydroxide dissolution in the presence of various types of DOM (e.g., Stumm and Furrer, 1987; Namjesnik-Dejanovic et al., 2000), although reductive dissolution is also possible. In contrast, exposure of the goethite to the irradiated sample increased Fe concentrations as Fe(II), suggesting reductive dissolution by the DOM or by some other photo-produced reductant, hence indicating a potential shift in dissolution mechanism. However, it is also possible that ligand-promoted reduction occurred through a non-reductive mechanism, followed by reduction of Fe(III) to Fe(II) in solution.

At pH 5.5, with non-irradiated DOM, total iron increased slightly during adsorption, indicating net dissolution (Fig. 8a). However, Fe(II) decreased during DOM sorption, suggesting Fe(II) sorption to the goethite surface (Zhang et al. 1992), or Fe(II) oxidation. In contrast, at pH 5.5 with irradiated DOM, Fe(II) and total Fe concentrations both decreased substantially

upon exposure to the goethite surface (Fig. 8b). Since Fe(II) was initially a larger fraction of the total iron in this case, this suggests that the Fe(II) generated by the irradiation process sorbed to the goethite surface. This sorbed Fe could either remain in its reduced oxidation state, or be oxidized at the surface. Other researchers have shown that iron oxyhydroxides can catalyze the oxidation of Fe(II) to Fe(III) (Sung and Morgan, 1980; Wehrli, 1990; Pullin and Cabaniss, 2003b). However, it is also possible that the Fe(II) was oxidized in solution, followed by precipitation or adsorption as either ionic Fe(III) or a Fe(III)-DOM complex, which would be indistinguishable from Fe(II) adsorption in our experiments.

It is important to note that our observations are probably the net result of a variety of dissolution and redox processes. It is likely that both adsorption and dissolution occurred at pH 3.5 and 5.5, but at pH 3.5, dissolution played a larger role in changing total dissolved Fe concentrations whereas at pH 5.5, adsorption played a more pronounced role.

5. CONCLUSIONS

- Adsorption of non-irradiated DOM was preferential to relatively high and intermediate molecular weight components at pH 3.5 and to intermediate molecular weight components at pH 5.5. Lack of adsorption of the highest molecular weight components at pH 5.5 may be due to electrostatic repulsion between these highly charged molecules and nearby adsorbed molecules. At pH 3.5, protonation would lead to more neutral molecules, hence stabilization by hydrophobic interactions.
- Irradiation substantially decreased adsorption at pH 3.5, primarily due to loss of components in the 1251—3750 and 3751–11350 Da fractions. Irradiation resulted in only a small decrease in DOM adsorption affinity at pH 5.5; the loss of components in the 3751–11350 Da fraction upon irradiation had little effect on adsorption because they played little or no role in the non-irradiated sample at this pH.
- The lack of significant adsorption of acetic, formic, and malonic acids can likely be attributed to the competition for surface sites by the DOM. On the other hand, oxalic acid adsorbed even in the presence of DOM, indicative of the exceptional adsorption affinity of iron oxides for this dicarboxylic acid.
- Irradiation of DOM also affected its interactions with iron in solution and at the goethite surface. For example, a possible shift in goethite dissolution mechanism (from ligand promoted to reductive) for the irradiated versus non-irradiated DOM was noted at pH 3.5. These effects on iron speciation (Fe(II) vs Fe(III)) are highly pH dependent. For example, it is likely that both adsorption and dissolution occurred at pH 3.5 and 5.5; but at pH 3.5, dissolution played a larger role in changing total dissolved Fe concentrations whereas at pH 5.5, adsorption played a more pronounced role.
- Overall, study results demonstrate that the combined effects of irradiation followed by adsorption produce a lower molecular weight, less aromatic DOM pool (based on a correlation between aromaticity and absorbance) than either process, alone. This could have important environmental consequences in terms of UV penetration, contaminant mobility, and DOM bioavailability.

Acknowledgments—The authors thank Notre Dame students Stephanie Golden and Charles Anthony for assistance with analyses. We thank the Center for Environmental Science and Technology and the Environmental Molecular Science Institute at Notre Dame for access to analytical equipment and the University of Notre Dame Environmental Research Center for field facilities. The comments of three reviewers greatly improved this manuscript, and are greatly appreciated. This research was funded by the National Science Foundation (Hydrologic Sciences).

REFERENCES

Albert D. B. and Martens C. S. (1997) Determination of low-molecular-weight organic acid concentrations in seawater and pore-samples via HPLC. *Marine Chem.* **56**, 27–37.

Benner R. and Opsahl S. (2001) Molecular indicators of the sources and transformations of dissolved organic matter in the Mississippi river plume. *Org. Geochem.* **32**, 597–611.

Bertilsson S. and Bergh S. (1999) Photochemical reactivity of XAD-4 and XAD-8 adsorbable dissolved organic compounds from humic waters. *Chemos.* **39**, 2289–2300.

Bertilsson S. and Tranvik L. J. (1998) Photochemically produced carboxylic acids as substrates for freshwater bacterioplankton. *Limnol. Oceanogr.* **43**, 885–895.

Bertilsson S. and Tranvik L. J. (2000) Photochemical transformation of dissolved organic matter in lakes. *Limnol. Oceanogr.* **45**, 753–762.

Cabaniss S. E., Zhou Q., Maurice P. A., Chin Y. and Aiken G. R. (2000) A log-normal distribution model for the molecular weight of aquatic fulvic acids. *Environ. Sci. Technol.* **34**, 1103–1109.

Chin Y. P., Aiken G. and O'Laughlin, E. (1994) Molecular weight, polydispersity, and spectroscopic properties of aquatic humic substances. *Environ. Sci. Technol.* **28**, 1853–1858.

Davis J. A. (1982) Adsorption of natural organic matter at the oxide/water interface. *Geochim. Cosmochim. Acta* **46**, 2381–2393.

Davis J. A. and Gloor R. (1981) Adsorption of dissolved organics in lake water by aluminum oxide. Effects of molecular weight. *Environ. Sci. Technol.* **15**, 1223–1229.

De la Rosa G., Peralta-Videa J. R. and Gardea-Torresdey J. L. (2003) Utilization of ICP/OES for the determination of trace metal binding to different humic fractions. *J. Hazard. Mater.* **B97**, 201–218.

De Laat A. W. M. and van den Heuval G. L. T. (1995) Molecular-weight fractionation in the adsorption of polyacrylic-acid salts onto $BaTiO_3$. *Colloid. Surf. A.* **98**, 53–59.

De Laat A. W. M., van den Heuval G. L. T. and Bohmer M. R. (1995) Kinetic aspects in the adsorption of polyacrylic salts onto $BaTiO_3$. *Colloid. Surf. A.* **98**, 61–71.

Faust B. C. and Zepp R. G. (1993) Photochemistry of aqueous iron(III)-polycarboxylate complexes: roles in the chemistry of atmospheric and surface waters. *Environ. Sci. Technol.* **27**, 2517–2522.

Filius J. D., Meeussen J. C. L., Lumsdon D. G., Hiemstra T., and van Riemsdijk W. H. (2003) Modeling the binding of fulvic acid by goethite: The speciation of adsorbed FA molecules. *Geochim. Cosmochim. Acta* **67**, 1463–1474.

Gao H. and Zepp R. G. (1998) Factors influencing photoreactions of dissolved organic matter in a coastal river of the southeastern United States. *Environ. Sci. Technol.* **32**, 2940–2946.

Goldberg M. C., Cunningham K. M. and Weiner E. R. (1993) Aquatic photolysis: photolytic reactions between goethite and adsorbed organic acids in aqueous solutions. *J. Photochem. Photobiol. A: Chem.* **73**, 105–120.

Goldstone J. V., Pullin M. J., Bertilsson S. and Voelker B. M. (2002) Reactions of hydroxyl radical with humic substances: Bleaching, mineralization, and production of bioavailable carbon substrates. *Environ. Sci. Technol.* **36**, 364–372.

Gu B., Schmitt J., Chen Z. and McCarthy J. F. (1994) Adsorption and desorption of natural organic matter on iron oxide: mechanisms and models. *Environ. Sci. Technol.* **28**, 38–46.

Gu B., Schmitt J., Chen Z., Liang L. and McCarthy J. F. (1995) Adsorption and desorption of different organic matter fractions on iron oxide. *Geochim. Cosmochim. Acta* **59**, 219–229.

Hernes P. J. and Benner R. (2003a) Transport and diagenesis of dissolved and particulate terrigenous organic matter in the North

Pacific Ocean. *Deep Sea Res. I: Oceanogr. Res. Papers.* **49**, 2119–2132.

Hernes P. J. and Benner R. (2003b). Photochemical and microbial degradation of dissolved lignin phenols: Implications for the fate of terrigenous dissolved organic matter in marine environments. *J. Geophys. Res.*, **108**.

Horányi G. (2002) Specific adsorption of simple organic acids on metal(hydr)oxides: A radiotracer approach. *J. Coll. Interf. Sci.* **254**, 214–221.

Hur J. and Schlautman M. A. (2003) Molecular weight fractionation of humic substances by adsorption to minerals. *J. Coll. Int. Sci.* **264**, 313–321.

Kaiser K. and Zech W. (1997) Competitive sorption of dissolved organic matter fractions to soils and related mineral phases. *Soil Sci. Soc. Am. J.* **61**, 64–69.

Kalbitz K., Schwesig D., Schmerwitz J., Kaiser K., Haumaier L., Glaser B., Ellerbrock R. and Leinweber P. (2003) Changes in properties of soil-derived dissolved organic matter induced by biodegradation. *Soil Biol. Biochem.* **35**, 1129–1142.

Kieber D. J. and Mopper K. (1987) Photochemical formation of glyoxylic and pyruvic acids in seawater. *Marine Chem.* **21**, 135–149.

Kieber R. J., Hardison D. R., Whitehead R. F. and Willey J. D. (2003) Photochemical production of Fe(II) in rainwater. *Environ. Sci. Technol.* **37**, 4610–4616.

Kieber R. J., Zhou X. and Mopper K. (1990) Formation of carbonyl compounds from UV-induced photodegradation of humic substances in natural waters: Fate of riverine carbon in the sea. *Limnol. Oceanogr.* **35**, 1503–1515.

Koopal L. K. (1981) The effect of polymer polydispersity on the adsorption isotherm. *J. Coll. Interf. Sci.* **83**, 116–129.

Lofts S. and Tipping E. (2000) Solid-solution metal partitioning in the Humber rivers: Application of WHAM and SCAMP. *Sci. Total Environ.* **251/252**, 381–399.

Maurice P. A., Cabaniss S. E., Drummond J. and Ito E. (2002a) Hydrogeochemical controls on the variations in chemical characteristics of natural organic matter at a small freshwater wetland. *Chem. Geol.* **187**, 59–77.

Maurice P. A., Pullin M. J., Cabaniss S. E., Zhou Q., Namjesnik-Dejanovic K. and Aiken G. R. (2002b) A comparison of surface water natural organic matter in raw filtered water samples, XAD, and reverse osmosis isolates. *Water Res.* **36**, 2357–2371.

McKnight D. M., Bencal a K. E., Zellweger G. W., Aiken G. R., Feder G. L. and Thorn K. A. (1992) Sorption of dissolved organic carbon by hydrous aluminum and iron oxides occurring at the confluence of deer creek with the Snake River, Summit county, Colorado. *Environ. Sci. Technol.* **26**, 1388–1396.

Meier M., Namjesnik-Dejanovik K., Maurice P. A., Chin Y.-P. and Aiken G. R. (1999) Fractionation of aquatic natural organic matter upon sorption to goethite and kaolinite. *Chem. Geol.* **157**, 275–284.

Miller W. L. and Moran M. A. (1997) Interaction of photochemical and microbial processes in the degradation of refractory dissolved organic matter from a coastal marine environment. *Limnol. Oceanogr.* **42**, 1317–1324.

Miwa H., Hiyama C. and Yamamoto M. (1985) High-performance liquid chromatography of short- and long-chain fatty acids as 2-nitrophenylhydrazides. *J. Chromatog.* **321**, 165–174.

Mopper K. and Stahovec W. L. (1986) Sources and sinks of low molecular weight organic carbonyl compounds in seawater. *Marine Chem.* **19**, 305–321.

Moran M. A. and Zepp R. G. (1997) Role of photoreactions in the formation of biologically labile compounds from dissolved organic matter. *Limnol. Oceanogr.* **42**, 1307–1316.

Moran M. A., Sheldon W. M. and Zepp R. G. (2000) Carbon loss and optical property changes during long-term photochemical and biological degradation of estuarine dissolved organic matter. *Limnol. Oceanogr.* **45**, 1254–1264.

Morris D. P. and Hargreaves B. R. (1997) The role of photochemical degradation of dissolved organic carbon in regulating the UV transparency of three lakes on the Pocono Plateau. *Limnol. Oceanogr.* **42**, 239–249.

Morris D. P., Zagarese H., Williamson C. E., Balseiro E. G., Hargreaves B. R., Modenutti B., Moeller R. and Queimalinos C. (1995) The attentuation of solar UV radiation in lakes and the role of dissolved organic carbon. *Limnol. Oceanogr.* **40**, 1381–1391.

Mueller-Harvey I. and Parkes R. J. (1987) Measurement of volatile fatty acids in pore water from marine sediments by HPLC. *Estuar., Coast., Shelf Sci.* **25**, 567–579.

Murphy E. M., Zachara J. M. and Smith S. C. (1990) Influence of mineral-bound humic substances on the sorption of hydrophobic organic compounds. *Environ. Sci. Technol.* **24**, 1507–1516.

Namjesnik-Dejanovic K., Maurice P. A., Aiken G. R., Cabaniss S. E., Chin Y. and Pullin M. J. (2000) Adsorption and fractionation of a muck fulvic acid on kaolinite and goethite at pH 3.7, 6, and 8. *Soil Sci.* **165**, 545–559.

Novak J. M., Mills G. L. and Bertsch P. M. (1992) Estimating the percent aromatic carbon in soil and aquatic humic substances using ultraviolet absorbance spectrometry. *J. Environ. Qual.* **21**, 144–147.

Pehkonen S. O., Slefert R., Erel Y., Webb S. and Hoffman M. R. (1993) Photoreduction of iron oxyhydroxides in the presence of important atmospheric organic compounds. *Env. Sci. Tech.* **27**, 2056–2062.

Peuravuori J. and Pihlaja K. (1997) Molecular distribution and spectroscopic properties of aquatic humic substances. *Anal. Chim. Acta* **337**, 133–149.

Progess C. (2003) Effects of photoirradiation on natural organic matter adsorption to goethite. unpub. M.S. thesis, University of Notre Dame.

Pullin M. J. and Cabaniss S. E. (1997) Physicochemical Variations in DOM-Synchronous Fluorescence: Implications for Mixing Studies. *Limnol. Oceanogr.* **42**, 1766–1773.

Pullin M. J. and Cabaniss S. E. (2001) Colorimetric flow-injection analysis of dissolved iron(II) and total iron in natural waters containing dissolved organic matter. *Water Res.* **35**, 363–372.

Pullin M. J. and Cabaniss S. E. (2003a) The effects of pH, ionic strength, and iron redox state on iron-fulvic acid interactions. II. The kinetics of complexation and dark reduction. *Geochim. Cosmochim. Acta* **67**, 4067–4077.

Pullin M. J. and Cabaniss S. E. (2003b) The effects of pH, ionic strength, and iron redox state on iron-fulvic acid interactions. I. Iron(II) oxidation and iron colloid formation. *Geochim. Cosmochim. Acta* **67**, 4079–4089.

Schulthess C. P. and Huang C. P. (1991) Humic and fulvic-acid adsorption by silicon and aluminum-oxide surfaces on clay-minerals. *Soil Sci. Soc. Am. J.* **55**, 34–42.

Schwertmann U., Cornell R. M. (1991) Iron oxides in the laboratory: Preparation and characterization. VCH.

Scott D. T., McKnight D. M., Blunt-Harris E. L., Kolesar S. E. and Lovley D. R. (1998) Quinone moieties act as electron acceptors in the reduction of humic substances by humics-reducing microorganisms. *Env. Sci. Technol.* **32**, 2984–2989.

Scully N. M., Lean D. R. S., McQueen D. J. and Cooper W. J. (1995) Photochemical formation of hydrogen peroxide in lakes: Effects of dissolved organic carbon and ultraviolet radiation. *Can. J. Fish. Aquat. Sci.* **52**, 2675–2681.

Serkiz S. M. and Perdue E. M. (1990) Isolation of dissolved organic-matter from the Suwannee River using reverse-osmosis. *Water Res.* **24**, 911–916.

Sigg L. and Stumm W. (1981) The interaction of anions and weak acids with the hydrous goethite (α-FeOOH) surface. *Colloid. Surf.* **2**, 101–117.

Southworth B. A. and Voelker B. M. (2003) Hydroxyl radical production via the photo-Fenton reaction in the presence of fulvic acid. *Environ. Sci. Technol.* **37**, 1130–1136.

Stumm W., Furrer G. (1987) The dissolution of oxides and aluminum silicates: Examples of surface-coordination-controlled kinetics. In *Aquatic Surface Chemistry* (ed. W.) Stumm, pp. 197–219. New York, John Wiley and Sons.

Stumm W. and Sulzberger B. (1992) The cycling of iron in natural environments: Considerations based on laboratory studies of heterogeneous redox processes. *Geochim. Cosmochim. Acta* **56**, 3233–3257.

Sun L., Perdue E. M. and McCarthy J. F. (1995) Using reverse-osmosis to obtain organic-matter from surface and ground waters. *Water Res.* **29**, 1471–1477.

Sung W. and Morgan J. J. (1980) Kinetics and product of ferrous iron oxygenation in aqueous systems. *Environ. Sci. Technol.* **14**, 561–568.

Tipping E. (1981) The adsorption of aquatic humic substances by iron oxides. *Geochim. Cosmochim. Acta* **45**, 191–199.

Tipping E. and Cooke D. (1982) The effects of adsorbed humic substances on the surface charge of goethite in freshwaters. *Geochim. Cosmochim. Acta* **46**, 75–80.

Tipping E., Rey-Castro C., Bryan S. E. and Hamilton-Taylor J. (2002) Al(III) and Fe(III) binding by humic substances in freshwaters, and implications for trace metal speciation. *Geochim. Cosmochim. Acta* **66**, 3211–3224.

Traina S. J., Novak J. and Smeck N. E. (1990) An ultraviolet absorbance method for estimating the percent aromatic carbon content of humic acids. *J. Environ. Qual.* **19**, 151–153.

Vermeer A. W. P., van Riemsdijk W. H. and Koopal L. K. (1998) Adsorption of humic acids to mineral particles. 1. Specific and electrostatic interactions. *Langmuir* **14**, 2810–2819.

Voelker B. M. and Sulzberger B. (1996) Effects of fulvic acid on Fe(II) oxidation by hydrogen peroxide. *Environ. Sci. Technol.* **30**, 1106–1114.

Voelker B. M., Morel F. M. M. and Sulzberger B. (1997) Iron redox cycling in surface waters: Effects of humic substances and light. *Environ. Sci. Technol.* **31**, 1004–1011.

Wehrli B. (1990) Redox reactions of metal ions at mineral surfaces. Chap. 11. In *Aquatic chemical kinetics: Reaction rates of processes in natural waters* (ed. W. Stumm), pp 311–336. Wiley-Interscience.

Weishaar J. L., Aiken G. R., Bergamaschi B. A., Fram M. S., Fujii R. and Mopper K. (2003) Evaluation of specific ultraviolet absorbance as an indicator of the chemical composition and reactivity of dissolved organic carbon. *Environ. Sci. Technol.* **37**, 4702–4708.

Wetzel R. G., Hatcher P. G. and Bianchi T. S. (1995) Natural photolysis by ultraviolet irradiance of recalcitrant dissolved organic matter to simple substrates for rapid bacterial metabilism. *Limnol. Oceanogr.* **40**, 1369–1380.

Wijnja H. and Schulthess C. P. (2002) Effect of carbonate on the adsorption of selenate and sulfate on goethite. *Soil Sci. Soc. Am. J.* **66**, 1190–1191.

Yan N. D., Keller W., Scully N. M., Lean D. R. S. and Dillon P. J. (1996) Increased UV-B penetration in a lake owing to drought-induced acidification. *Nature* **381**, 141–143.

Zepp R. G., Callaghan T. V. and Erickson D. J. (1998) Effects of enhanced solar ultraviolet radiation on biogeochemical cycles. *J. Photochem. Photobiol. B: Biol*. **46**, 69–82.

Zhang Y., Charlet L. and Schindler P. W. (1992) Adsorption of protons, Fe(II) and Al(III) on lepidocrocite. *Colloids Surf.* **63**, 259–268.

Zhou Q., Cabaniss S. E. and Maurice P. A. (2000) Considerations in the use of high-pressure size exclusion chromatography (HPSEC) for determining molecular weights of aquatic humic substances. *Water Res.* **34**, 3505–3514.

Zhou Q., Maurice P. A. and Cabaniss S. E. (2001) Size fractionation upon adsorption of fulvic acid on goethite: Equilibrium and kinetic studies. *Geochim. Cosmochim. Acta* **65**, 803–812.